

# 1,2,4-Triazole-3-Thione Analogues with a 2-Ethylbenzoic Acid at Position 4 as VIM-type Metallo- $\beta$ -Lactamase Inhibitors

Federica Verdirosa<sup>+</sup>,<sup>[a]</sup> Laurent Gavara<sup>+</sup>,<sup>\*[b]</sup> Laurent Seville,<sup>[b]</sup> Giusy Tassone,<sup>[c]</sup> Giuseppina Corsica,<sup>[a]</sup> Alice Legru,<sup>[b]</sup> Georges Feller,<sup>[d]</sup> Giulia Chelini,<sup>[a]</sup> Paola Sandra Mercuri,<sup>[e]</sup> Silvia Tanfoni,<sup>[a]</sup> Filomena Sannio,<sup>[a]</sup> Manuela Benvenuti,<sup>[c]</sup> Giulia Cerboni,<sup>[a]</sup> Filomena De Luca,<sup>[a]</sup> Ezeddine Bouajila,<sup>[b]</sup> Yen Vo Hoang,<sup>[b]</sup> Patricia Licznar-Fajardo,<sup>[f]</sup> Moreno Galleni,<sup>[e]</sup> Cecilia Pozzi,<sup>[c]</sup> Stefano Mangani,<sup>[c]</sup> Jean-Denis Docquier,<sup>\*[a, g]</sup> and Jean-François Hernandez<sup>\*[b]</sup>

Metallo- $\beta$ -lactamases (MBLs) are increasingly involved as a major mechanism of resistance to carbapenems in relevant opportunistic Gram-negative pathogens. Unfortunately, clinically efficient MBL inhibitors still represent an unmet medical need. We previously reported several series of compounds based on the 1,2,4-triazole-3-thione scaffold. In particular, Schiff bases formed between diversely 5-substituted-4-amino compounds and 2-carboxybenzaldehyde were broad-spectrum inhibitors of VIM-type, NDM-1 and IMP-1 MBLs. Unfortunately, these compounds were unable to restore antibiotic susceptibility of MBL-producing bacteria, probably because of poor penetration and/or susceptibility to hydrolysis. To improve their microbiological activity, we synthesized and characterized compounds where the hydrazone-like bond of the Schiff base

analogues was replaced by a stable ethyl link. This small change resulted in a narrower inhibition spectrum, as all compounds were poorly or not inhibiting NDM-1 and IMP-1, but showed a significantly better activity on VIM-type enzymes, with  $K_i$  values in the  $\mu\text{M}$  to sub- $\mu\text{M}$  range. The resolution of the crystallographic structure of VIM-2 in complex with one of the best inhibitors yielded valuable information about their binding mode. Interestingly, several compounds were shown to restore the  $\beta$ -lactam susceptibility of VIM-type-producing *E. coli* laboratory strains and also of *K. pneumoniae* clinical isolates. In addition, selected compounds were found to be devoid of toxicity toward human cancer cells at high concentration, thus showing promising safety.

## Introduction

Main Bacterial resistance to antibiotics significantly increased during the last decades, with the growing spread of clinical isolates showing multidrug-, or even pandrug-, resistance phenotypes. This global issue is now recognized as a very serious threat to Public Health and needs response to be urgently

addressed, including with the discovery and development of new antibacterial drugs active against antibiotic-resistant opportunistic pathogens.<sup>[1,2]</sup> The World Health Organization (WHO) previously disclosed a list of “priority pathogens for R&D of new antibiotics”, and identified multidrug- and extensively-drug resistant Gram-negative bacteria responsible of life-threatening nosocomial infections as a critical priority. Indeed, carbapenem-

[a] F. Verdirosa,<sup>+</sup> G. Corsica, G. Chelini, S. Tanfoni, F. Sannio, G. Cerboni, Dr. F. De Luca, Prof. J.-D. Docquier  
Dipartimento di Biotecnologie Mediche  
Università di Siena, 53100 Siena (Italy)  
E-mail: jddocquier@unisi.it

[b] Dr. L. Gavara,<sup>+</sup> Dr. L. Seville, Dr. A. Legru, Dr. E. Bouajila, Dr. Y. Vo Hoang, Dr. J.-F. Hernandez  
IBMM, CNRS, Univ Montpellier, ENSCM, Montpellier (France)  
E-mail: laurent.gavara@umontpellier.fr  
jean-francois.hernandez@umontpellier.fr

[c] Dr. G. Tassone, Dr. M. Benvenuti, Prof. C. Pozzi, Prof. S. Mangani  
Dipartimento di Biotecnologie, Chimica e Farmacia  
Università di Siena, 53100 Siena (Italy)


[d] Dr. G. Feller  
Laboratoire de Biochimie, Centre d'Ingénierie des Protéines-InBioS  
Université de Liège  
Allée du 6 août B6, Sart-Tilman, 4000 Liège (Belgium)


[e] Dr. P. S. Mercuri, Prof. M. Galleni  
Laboratoire des Macromolécules Biologiques, Centre d'Ingénierie des Protéines-InBioS  
Université de Liège  
Institute of Chemistry B6a, Sart-Tilman, 4000 Liège (Belgium)

[f] Dr. P. Licznar-Fajardo  
HSM, Univ Montpellier  
CNRS, IRD, CHU Montpellier, Montpellier (France)

[g] Prof. J.-D. Docquier  
Centre d'Ingénierie des Protéines-InBioS  
Université de Liège, 4000 Liège (Belgium)

[\*] These authors contributed equally to this work.

 Supporting information for this article is available on the WWW under <https://doi.org/10.1002/cmdc.202100699>

 © 2022 The Authors. ChemMedChem published by Wiley-VCH GmbH. This is an open access article under the terms of the Creative Commons Attribution Non-Commercial NoDerivs License, which permits use and distribution in any medium, provided the original work is properly cited, the use is non-commercial and no modifications or adaptations are made.

resistant *Acinetobacter baumannii*, *Pseudomonas aeruginosa* and Enterobacterales represent the primary focus of many antibacterial discovery and development programs.<sup>[3,4]</sup>

Carbapenems are extremely valuable drugs, used as last-resort antibiotics for the treatment of infections caused by multidrug-resistant clinical isolates. Therefore, substantial efforts to restore their efficacy, e.g. with the use of  $\beta$ -lactamase inhibitors active on carbapenem-hydrolyzing  $\beta$ -lactamases, are considered extremely worthy. The major mechanism of carbapenem resistance relies on the production of carbapenemases, i.e.  $\beta$ -lactamases able to inactivate these antibiotics as well as, usually, both penicillins and cephalosporins via hydrolysis of their  $\beta$ -lactam ring.<sup>[5-7]</sup> Considered as major therapeutic targets, they belong to several molecular classes, such as class A (e.g. KPC-type enzymes) and D (e.g. OXA-48, OXA-24/40) serine- $\beta$ -lactamases (SBLs),<sup>[8]</sup> or class B metallo- $\beta$ -lactamases (MBLs). To date, while SBL inhibitors targeting KPC- and OXA-48-type carbapenemases (i.e. avibactam and vaborbactam) have been recently marketed,<sup>[9,10]</sup> no MBL inhibitor has been approved yet.

MBLs are further subdivided into subclasses B1, B2, and B3.<sup>[11]</sup> Subclasses B1 and B3 MBLs are generally di-zinc enzymes while subclass B2 MBLs are active only as monozinc species. Acquired MBLs are found in many Gram-negative bacteria of high clinical relevance, which primarily correspond to the above-mentioned WHO critical priority list. Acquired subclass B1 MBLs are carbapenemases with an exceedingly broad substrate profile and include the most clinically relevant enzymes, such as the VIM-, NDM-, and IMP-types. The global spread of MBL-producing isolates, not only in the hospital setting but also in the community, makes these enzymes particularly worrying.<sup>[12,13]</sup>

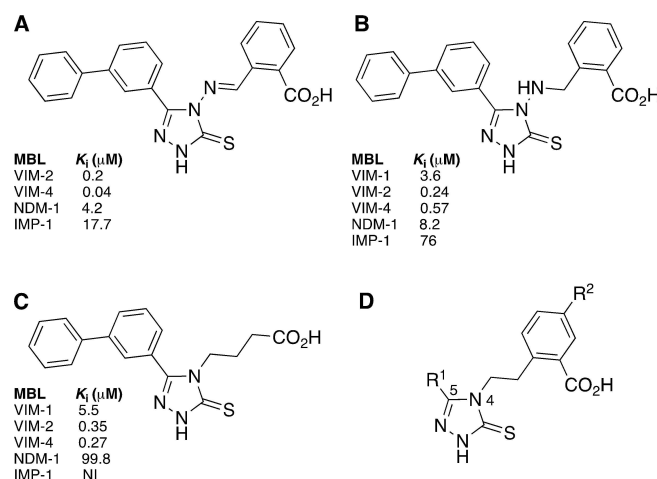
In fact, because there are several clinically important MBLs and the structural differences between VIM-, NDM- and IMP-type enzymes are significant it is difficult to discover a broad-spectrum inhibitor.<sup>[9,14,15]</sup> In addition, the most typical strategy for metallo-enzyme inhibition is to develop molecules with a zinc-coordinating group, which often predominantly accounts for binding strength. Therefore, there is a potential risk to face difficulties attaining sufficient selectivity toward important human metallo-enzymes.<sup>[16]</sup>

This risk likely exists with the largest families of reported MBL inhibitors, which contain a thiol group<sup>[17-19]</sup> or at least two carboxylate groups (e.g. succinate<sup>[20]</sup> and dipicolinate<sup>[21]</sup> analogues) as zinc ligand(s). A similar lack of selectivity could also be a potential limitation for Zn-chelating MBL inhibitors as aspergillomarasmine<sup>[22-24]</sup> or Zn148,<sup>[25]</sup> which act by stripping zinc ions from the active site. To date, the most promising inhibitors<sup>[26]</sup> are the thiazole-carboxylic acid ANT2681<sup>[27]</sup> and the cyclic boronates taniborbactam and QPX7728,<sup>[28-34]</sup> the latter showing unusual inhibitory activity on both MBLs and SBLs families. Taniborbactam and QPX7728 are today, respectively, under phase 3 and 1 of clinical development.<sup>[35]</sup>

We initiated a discovery and optimization program of MBL inhibitors based on the 1,2,4-triazole-3-thione scaffold, after the discovery by Otto Dideberg's group of its original binding mode in the active site of the di-zinc subclass B3 MBL L1, i.e. a simultaneous coordination of the two Zn ions by the N<sup>2</sup> (Zn1) and S<sup>3</sup> (Zn2) atoms of the heterocyclic moiety.<sup>[36]</sup> A similar

binding mode was more recently reported in the case of the di-zinc subclass B1 MBLs VIM-2<sup>[37-39]</sup> and NDM-1.<sup>[39]</sup> It is also noteworthy that several studies reporting random virtual and experimental screenings for MBL inhibition retrieved compounds containing this heterocycle in the case of L1,<sup>[40]</sup> IMP-1,<sup>[41]</sup> VIM-2<sup>[37,39]</sup> and NDM-1.<sup>[39,42]</sup> Overall, these studies suggest that molecules based on this scaffold have the potential to deliver broad-spectrum MBL inhibitors.

We confirmed this assumption with the synthesis of a first series of analogues diversely substituted at position 5 and substituted or not at position 4 by a NH<sub>2</sub> group.<sup>[43]</sup> Although their activities were generally modest and no compound showed  $\beta$ -lactam antibiotic protection in microbiological assays, some analogues inhibited a panel of representative MBLs (e.g. VIM-2, NDM-1, IMP-1) with IC<sub>50</sub> values in the micromolar range. We also synthesized a series of Schiff base analogues formed between the most interesting 5-substituted-4-amino-1,2,4-triazole-3-thiones and diversely substituted benzaldehydes (Figure 1A).<sup>[38]</sup> Broad-spectrum inhibition was maintained, while the presence of an aryl substituent attached at the position 4 of the heterocycle by a hydrazone-like bond significantly improved their potency. In particular, several favourable aryl groups (e.g. *o*-benzoic group) were identified. However, despite this higher potency, their synergistic antibacterial activity was quite disappointing. The main reason was very probably their insufficient ability to cross the bacterial outer membrane. Another reason might be the susceptibility of the hydrazone-like bond to hydrolysis. Therefore, we developed analogues in which this N=C double bond was replaced by a stable link. One series of molecules contained a hydrazine-like bond, which was obtained by reduction of the parent Schiff base analogues (Figure 1B).<sup>[44]</sup> However, although similar inhibitory activities were measured, this series was of limited interest because these compounds did not behave more favorably in microbiological assays. In parallel, we developed



**Figure 1.** Structure of previously reported 1,2,4-triazole-3-thione compounds with a carboxylic group on the 4-substituent and their inhibitory potency on selected MBLs: (A) Schiff base analogue,<sup>[38]</sup> (B) reduced Schiff base analogue,<sup>[44]</sup> (C) alkanolic analogue,<sup>[45]</sup> (D) general structure of synthesized analogues with a 2-ethylbenzoic acid substituent at position 4. NI: no inhibition.

another series of stable compounds possessing diversely substituted alkyl chains at position 4 and found that an alkanolic chain was favourable to VIM-type MBL inhibition (Figure 1C).<sup>[45]</sup> Most importantly, some compounds showed antibiotic potentiation activity on VIM-producing *K. pneumoniae* clinical isolates. Unfortunately, these compounds were characterized by a narrower inhibition spectrum as they were poorly or not active against NDM-1 and IMP-1, possibly accounting for the absence of an aromatic group in the 4-substituent. This was recently confirmed with a series of compounds substituted at the 4-position by a thioether-containing alkyl chain bearing an aryl group at its extremity, which showed a broader spectrum of activity.<sup>[46]</sup>

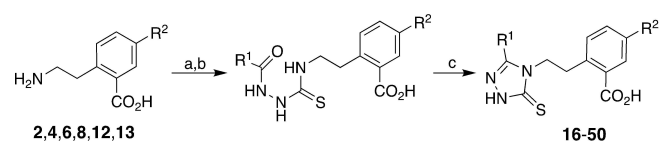
We herein report on a new series of stable analogues of 1,2,4-triazole-3-thione-based Schiff base inhibitors where the N–C double bond was replaced by an ethyl link bearing an *o*-benzoic acid group (Figure 1D). Whereas the compounds showed an inhibition spectrum limited to VIM-type enzymes (as with the 4-alkanoic series), the change to an alkyl link was again found to be significantly beneficial for their antibacterial synergistic activity.

## Results and Discussion

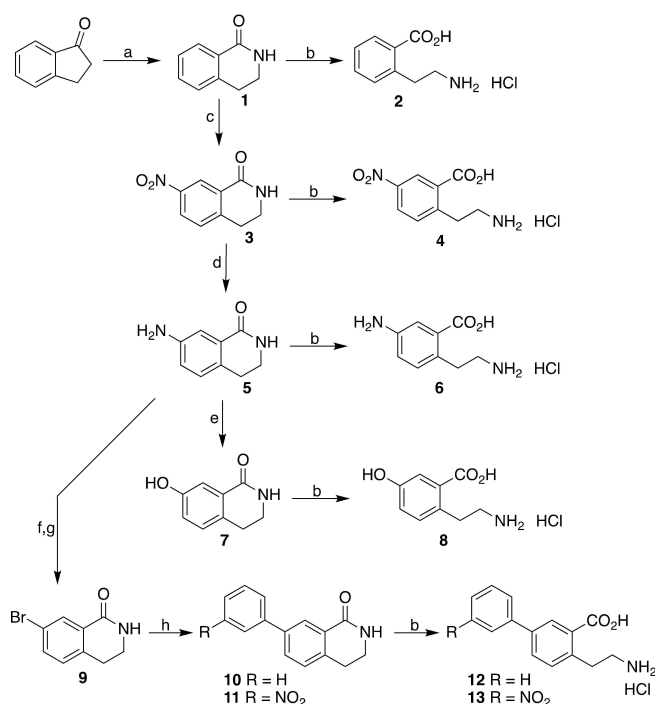
### Chemical synthesis

The synthesis of all compounds followed the pathway reported by Deprez-Poulain *et al.* (Scheme 1).<sup>[47]</sup> Amines **2**, **4**, **6**, **8**, **12** and **13** were treated with dipyridylthionocarbonate (DPT) to yield the intermediate isothiocyanates, which were directly reacted with hydrazides R<sup>1</sup>-CONHNH<sub>2</sub> to form the thiosemicarbazide derivatives. Their basic treatment yielded the expected 1,2,4-triazole-3-thione compounds.

The 2-(2-aminoethyl)benzoic acid precursors of substituent at position 4 (**2**, **4**, **6**, **8**, **12**, **13**) were prepared as described in Scheme 2. The 2-(2-aminoethyl)benzoic acid **2** was obtained from indanone in two steps. The indanone was treated with sodium azide in concentrated HCl to yield the 3,4-dihydro-1(2*H*)-isoquinolinone **1**,<sup>[48]</sup> which was opened in concentrated HCl at 110 °C to yield the amine **2**.<sup>[49]</sup> All other amines were synthesized from 3,4-dihydro-7-nitro-1(2*H*)-isoquinolinone (**3**). Compound **3** was obtained by selective nitration of **1** using fuming nitric acid in sulfuric acid. The lactam **3** was opened as described to yield the amine **4**. The nitro group of **3** was also reduced to the aromatic amine **5**, which was hydrolyzed to yield the amine **6**. Compound **5** was subjected to diazotation followed by treatment



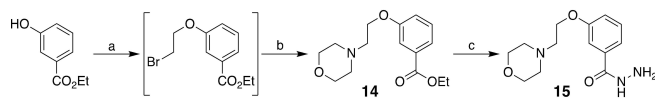
**Scheme 1.** Synthesis of 4-[(2-carboxy-phenyl)eth-2-yl]-1,2,4-triazole-3-thione derivatives. Reagents and conditions: (a) DPT, DMF, 55 °C, 3 h; (b) R<sup>1</sup>-CONHNH<sub>2</sub>, DMF, 55 °C, 3 h; (c) aqueous KOH or NaHCO<sub>3</sub>, 100 °C, 3 h.



**Scheme 2.** Synthesis of the 2-(2-aminoethyl)benzoic acids precursors R<sup>2</sup>-NH<sub>2</sub> **2**, **4**, **6**, **8**, **12**, **13**. Reagents and conditions: (a) Conc. HCl, NaN<sub>3</sub>, rt, 15 h; (b) Conc. HCl, 110 °C, 15 h; (c) Fuming HNO<sub>3</sub>, H<sub>2</sub>SO<sub>4</sub>, 0 °C, 1 h 30; (d) H<sub>2</sub>, 10% Pd/C, rt, 8 h; (e) H<sub>2</sub>SO<sub>4</sub>, NaNO<sub>2</sub>, water, 0 °C, 40 min, +90 °C, 1 h 30; (f) 48% HBr, NaNO<sub>2</sub>, water, 0 °C, 30 min; (g) CuBr, rt, 30 min +70 °C, 1 h; (h) phenylboronic acid or 3-nitro-phenylboronic acid, 2 M aq. Na<sub>2</sub>CO<sub>3</sub>, toluene/MeOH, tetrakis, reflux, 4 h.

with water or CuBr to respectively yield the phenol **7** and the brominated compound **9**. Compound **7** was hydrolyzed to give the amine **8**. Finally, compound **9** was subjected to Suzuki coupling with either phenylboronic acid or its 3-nitro derivative to yield compounds **10** and **11**, respectively. Hydrolysis of **10** and **11** led to the corresponding amines **12** and **13**.

When not commercially available, the hydrazides R<sup>1</sup>-CONHNH<sub>2</sub> were obtained in two steps from the corresponding commercially available carboxylate derivatives R<sup>1</sup>-CO<sub>2</sub>H via the ethyl ester followed by hydrazine treatment as previously described,<sup>[44]</sup> excepted the hydrazides precursors of compounds **28** and **29**. The synthesis of the hydrazide **15** (precursor of **28**) is shown in Scheme 3 as an example. It was obtained from ethyl 3-hydroxybenzoate, which was reacted with 1,2-dibromoethane to give the halide intermediate, followed by substitution with morpholine (ester **14**) and hydrazine treatment.



**Scheme 3.** Synthesis of the hydrazide precursor **15**. Reagents and conditions: (a) 1,2-Dibromoethane, K<sub>2</sub>CO<sub>3</sub>, DMF, 100 °C, 6 h; (b) morpholine, DMF, 100 °C, 1 h; (c) hydrazine, EtOH, reflux, 3 h.

## Evaluation of inhibitory potency toward purified MBLs.

Compounds were tested against five representative, highly clinically relevant MBLs, i.e. the subclass B1 enzymes VIM-1, VIM-2, VIM-4, NDM-1 and IMP-1. Initially, testing was performed at a single concentration (100 or 200  $\mu\text{M}$ ) and  $K_i$  values were measured for compounds exhibiting  $>75\%$  inhibition. The results obtained for a series of 35 compounds are presented in Table 1. All possessed a 2-ethyl-benzoic group at position 4 and a variable aryl or aryl-alkyl substituent at position 5, excepted **50**, which displayed a cyclohexyl group. In the case of compound **16** ( $R^1$ =phenyl), the 2-ethyl-benzoic group was also diversely substituted at the para position of the ethyl group (**17–20**). A nitro group was similarly introduced on compound **21** ( $R^1$ =*o*-toluyl) giving **22**. However, no drastic change in activity was induced by any of these substitutions, although a slight decrease in inhibitory potency was generally observed when compared to the parent compounds **16** and **21**, suggesting that a substituent at this position was poorly relevant for interacting with the enzyme active site residues.

Overall, a large proportion of compounds significantly inhibited ( $K_i$  values  $< 15 \mu\text{M}$ ) at least one VIM-type enzyme, while NDM-1 and IMP-1 were only poorly or not inhibited. Among tested VIM-type enzymes, VIM-2 appeared to be the most sensitive enzyme, with  $K_i$  values commonly in the sub-micromolar range.

Compared to their corresponding analogues in the Schiff base series (i.e. same substituent at position 5), the compounds generally showed similar inhibitory potencies, either high (**16**, **21**, **27**, **44**) or low (**41**, **42**) against VIM-2 and VIM-4, but with some exceptions (i.e. **23–25**, **38**, **46–48**). Indeed, in contrast to the corresponding Schiff base analogues, the presence of halogen substituents in  $R^1$  was not favourable (i.e. **23–25**). Furthermore, the compounds with the  $R^1$  aryl group remote from the triazole ring by one or two  $\text{CH}_2$  were all inactive (i.e. **45–49**).

So, in the present series, high inhibitory potency against VIM-2 and VIM-4 enzymes ( $K_i < 5 \mu\text{M}$ ) was observed for compounds where the  $R^1$  group was either an unsubstituted phenyl ring (**16**, **17**), a phenyl substituted with a methyl group (**21**), an alkoxy group (**26–29**), a heteroaryl (**31–36**), or a biaryl (**38**, **40**, **43**, **44**), all (excepted unprecedented  $R^1$  substituent of **28** and **29**) shown to be favourable in previous Schiff base and/or alkanolic series.<sup>[38,45]</sup> In particular, replacing the phenyl ring of **16** by a hetero-pentacycle, including its thiophene bioisostere (i.e. **34–36**), was well tolerated with the exception of 4-methyl-1,2,3-thiadiazole as compound **37** was inactive against all tested MBLs. Compounds with a fused bicycle also displayed similar  $K_i$  values against VIM-2 and VIM-4 (i.e. **38**, **40**) as compound **16**, but loss of activity toward VIM-2 (i.e. **39**, **41**) or both VIM-2 and VIM-4 (i.e. **41**) was observed when a nitrogen was introduced at position ortho to the triazole ring. This effect was not observed when the nitrogen was distal (i.e. **40**). In the case of compounds with a biphenyl substituent, the relative orientation of the two phenyl rings (ortho for **42**, meta for **43**) was crucial as only the meta orientation (i.e. **43**) was favorable, suggesting that bringing the distal phenyl moiety closer to the triazole ring may hinder proper interaction with the dizinc active site. Compound **43** was the

most active against VIM-2 ( $K_i$  value of 80 nM). Its *m*-biphenyl substituent was shown the most favourable at position 5 in any 1,2,4-triazole-3-thione series that we synthesized. However, the docking study of one of these previous compounds (compound **60** in [45]) in the VIM-2 active site did not establish the existence of a particular interaction for this bulky aromatic moiety. Its effect might be indirect through its higher rigidity and/or the displacement of water molecules, which would contribute a favorable entropic stabilization energy.<sup>[45]</sup> Finally, replacing the phenyl ring by a cyclohexyl group (i.e. **50**) led to a large decrease in inhibitory potency, confirming the importance of an aromatic group at this position.

All potent VIM-2/4 inhibitors were generally less active against VIM-1, some being not or poorly active (**16**, **17**, **19**, **34**, **38**, **44**) and others showing  $K_i$  values in the 6–15  $\mu\text{M}$  range (**21**, **22**, **26–27**, **31–33**, **35**, **36**, **39**, **40**). While these results indicated significant structural variations between the binding sites of VIM-1 and VIM-2/4, they do not allow to extract precise rules for VIM-1 binding, except that the aryl substituent at position 5 should be a substituted phenyl group or an heteroaryl. Only four compounds (**28–30**, **43**) showed low micromolar activity against VIM-1. Among them, the most interesting compounds were **28**, **29** and **43**, which potently inhibited both VIM-type enzymes.

Interestingly, compounds **28** and **29** are characterized by a rather long meta substituent on their  $R^1$  phenyl group, an ethoxy group ending with a morpholine or *N*-methyl-piperazine moiety, respectively. Considering the  $\text{p}K_a$  values of these groups, they could bear a positive charge at neutral pH, which would advantageously allow an electrostatic interaction with the negatively charged region flanking the active site in VIM-2, and formed by residues Glu149 and Asp236 (conserved in VIM-1 and VIM-4), as observed for the positively-charged side chain of taniborbactam.<sup>[31]</sup> However, and when compared to their *m*-methoxyphenyl analogue **26**, compound **28** did not show significantly better inhibitory potency against VIM-2 and VIM-4, suggesting that the morpholinyl extension did not establish additional favorable interaction. In fact, this was supported by the analysis of the X-ray VIM-2/**28** three-dimensional structure (*vide infra*). In contrast, compound **29** was 3- to 4-fold and 5-fold better than **26** against VIM-2 and VIM-4, respectively. Also, **29** was 3-fold better than **28** on both enzymes and, interestingly, also on VIM-1. Therefore, we might argue that the replacement of the morpholinyl oxygen by a tertiary amine in **29** was responsible of this limited but significant improvement in affinity. Its basic character and/or the presence of a hydrogen bond donor would allow the *N*-methyl-piperazinyl moiety more favorably interacting with the negatively charged region flanking the active site in VIM-type enzymes. The 3D-structure of a complex VIM-2/**29** would be necessary to confirm this hypothesis.

Strikingly, most of the tested compounds did not significantly inhibit either NDM-1 or IMP-1. A single compound, **38** ( $R^1$ =naphth-2-yl), allowed to measure a  $K_i$  value of approximately 75  $\mu\text{M}$  against IMP-1, well above the typical  $K_i$  values obtained with other compounds on VIM-type enzymes. This result is in contrast with the activities measured for their Schiff base analogues (Figure 1A).<sup>[38]</sup> Indeed, whereas a few of the latter

**Table 1.** Inhibitory activity of 1,2,4-triazole-3-thiones 16–50 against various MBLs.

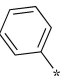
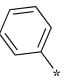
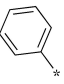
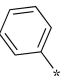
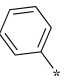
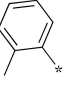
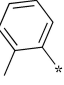
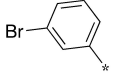
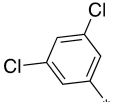
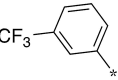
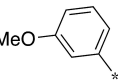
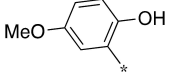
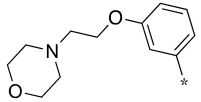
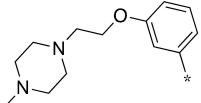
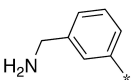
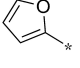
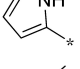
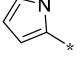
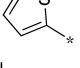
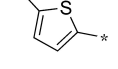
Cpd	R <sup>1</sup>	Structure	R <sup>2</sup>	VIM-1	K <sub>i</sub> [μM] <sup>[a]</sup> or (% inhibition at 100 <sup>[b]</sup> or 200 <sup>[c]</sup> μM)			IMP-1
					VIM-2	VIM-4	NDM-1	
16			H	NI <sup>[d]</sup>	0.25 ± 0.04	1.5 ± 0.15	NI	NI
17			OH	(36%) <sup>[b]</sup>	1.27 ± 0.06	4.06 ± 0.32	NI	(58%) <sup>[b]</sup>
18			NO <sub>2</sub>	NI	(45%) <sup>[b]</sup>	1.98 ± 0.09	NI	NI
19			NH <sub>2</sub>	(52%) <sup>[b]</sup>	2.26 ± 0.10	6.17 ± 0.43	NI	NI
20			Ph	(48%) <sup>[b]</sup>	(70%) <sup>[b]</sup>	(66%) <sup>[b]</sup>	(53%) <sup>[b]</sup>	(52%) <sup>[b]</sup>
21			H	6.41 ± 0.89	0.58 ± 0.19	5.16 ± 0.44	NI	NI
22			NO <sub>2</sub>	12.4 ± 1.2	1.61 ± 0.08	2.48 ± 0.24	NI	NI
23			H	NI	(49%) <sup>[b]</sup>	(36%) <sup>[b]</sup>	NI	NI
24			H	NI	(40%) <sup>[b]</sup>	NI	NI	(37%) <sup>[b]</sup>
25			H	NI	NI	NI	NI	NI
26			H	7.65 ± 0.67	0.38 ± 0.02	2.33 ± 0.10	NI	NI
27			H	7.55 ± 0.21	0.15 ± 0.07	2.01 ± 0.13	NI	NI
28			H	4.69 ± 0.24	0.34 ± 0.02	1.27 ± 0.06	NI	NI
29			H	1.60 ± 0.06	0.110 ± 0.004	0.47 ± 0.01	NI	NI
30			H	4.67 ± 0.25	2.47 ± 0.14	NI	NI	NI
31			H	8.08 ± 0.61	0.58 ± 0.19	3.07 ± 0.31	NI	NI
32			H	15.5 ± 0.8	2.09 ± 0.24	3.55 ± 0.35	NI	NI
33			H	10.2 ± 0.8	0.55 ± 0.12	2.86 ± 0.19	NI	NI
34			H	NI	1.07 ± 0.11	1.02 ± 0.06	NI	NI
35			H	8.71 ± 0.44	1.05 ± 0.15	1.80 ± 0.12	NI	NI

Table 1. continued

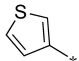

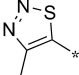

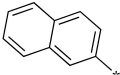

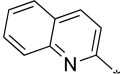

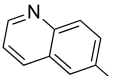

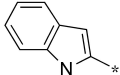

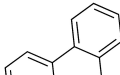

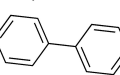

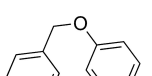

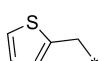

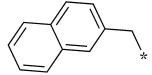
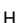
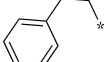

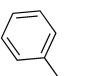

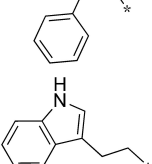

Cpd	R <sup>1</sup>	Structure	R <sup>2</sup>	K <sub>i</sub> [μM] <sup>[a]</sup> or (% inhibition at 100 <sup>[b]</sup> or 200 <sup>[c]</sup> μM)				IMP-1
				VIM-1	VIM-2	VIM-4	NDM-1	
36			H	9.19 ± 0.80	1.96 ± 0.13	2.39 ± 0.14	NI	NI
37			H	NI	NI	NI	NI	NI
38			H	NI	0.88 ± 0.06	3.30 ± 0.28	(60%) <sup>[c]</sup>	75.6 ± 6.3
39			H	6.07 ± 0.24	NI	1.65 ± 0.13	NI	NI
40			H	11.5 ± 0.34	1.14 ± 0.08	3.15 ± 0.17	NI	NI
41			H	NI	NI	NI	NI	NI
42			H	NI	NI	(30%) <sup>[b]</sup>	NI	NI
43			H	1.61 ± 0.30	0.08 ± 0.02	2.10 ± 0.54	NI	NI
44			H	(32%) <sup>[b]</sup>	0.19 ± 0.01	1.40 ± 0.27	NI	NI
45			H	NI	(30%) <sup>[b]</sup>	NI	NI	NI
46			H	NI	NI	NI	NI	NI
47			H	NI	(50%) <sup>[c]</sup>	NI	NI	NI
48			H	NI	NI	NI	NI	(45%) <sup>[b]</sup>
49			H	NI	NI	NI	NI	NI

Table 1. continued									
Cpd	R <sup>1</sup>	Structure	R <sup>2</sup>	VIM-1	K <sub>i</sub> [μM] <sup>[a]</sup> or (% inhibition at 100 <sup>[b]</sup> or 200 <sup>[c]</sup> μM)	VIM-2	VIM-4	NDM-1	IMP-1
50			H	(31%) <sup>[b]</sup>	NI	NI	(40%) <sup>[b]</sup>	NI	NI

[a] K<sub>i</sub> values were determined when inhibition > 75% and values are mean ± SD. Assays performed in triplicate; [b] % inhibition at 100 μM; [c] % inhibition at 200 μM. Kinetics were monitored at 30 °C by following the absorbance variation observed upon substrate hydrolysis. [d] NI: no inhibition (< 30% or < 50% inhibition at 100 or 200 μM, respectively).

analogues were modest but better IMP-1 inhibitors, a large number of compounds inhibited NDM-1 with K<sub>i</sub> values in the micromolar range. In particular, biaryl R<sup>1</sup> substituents were highly favourable in the hydrazone-like series, but it was not the case in the present series. For instance, the Schiff base analogues of the inactive compounds **38**, **43**, **44**, **46** and **48** showed K<sub>i</sub> values between 1.6 and 4.2 μM against NDM-1. A similar decrease in NDM-1 and IMP-1 inhibitory potency was also observed when reducing the hydrazone-like bond (Figure 1B) but a micromolar K<sub>i</sub> value could be measured for the corresponding analogue of **43** (R<sup>1</sup> = *m*-biphenyl).<sup>[44]</sup> In fact, the results obtained with the present series are comparable to those obtained with the alkanolic series (Figure 1C). Indeed, none of these, which possessed the same R<sup>1</sup> substituents, potently inhibited NDM-1 and IMP-1.<sup>[45]</sup> Taken together, these results confirmed that the replacement of the N–C double bond of the Schiff base analogues by an ethyl group was deleterious to NDM-1 inhibition. This might be due to the different geometry and higher flexibility of the link between the triazole ring and the phenyl group and/or to the elimination of a potential H-bond acceptor.

### Isothermal calorimetry (ITC) experiments

To validate the binding mode of compounds to VIM-2, ITC experiments were performed with compound **16** and **43**. The thermodynamic parameters of binding are given in Table 2 and Figure 2A. ITC thermograms are shown in Figures 2B and 2C.

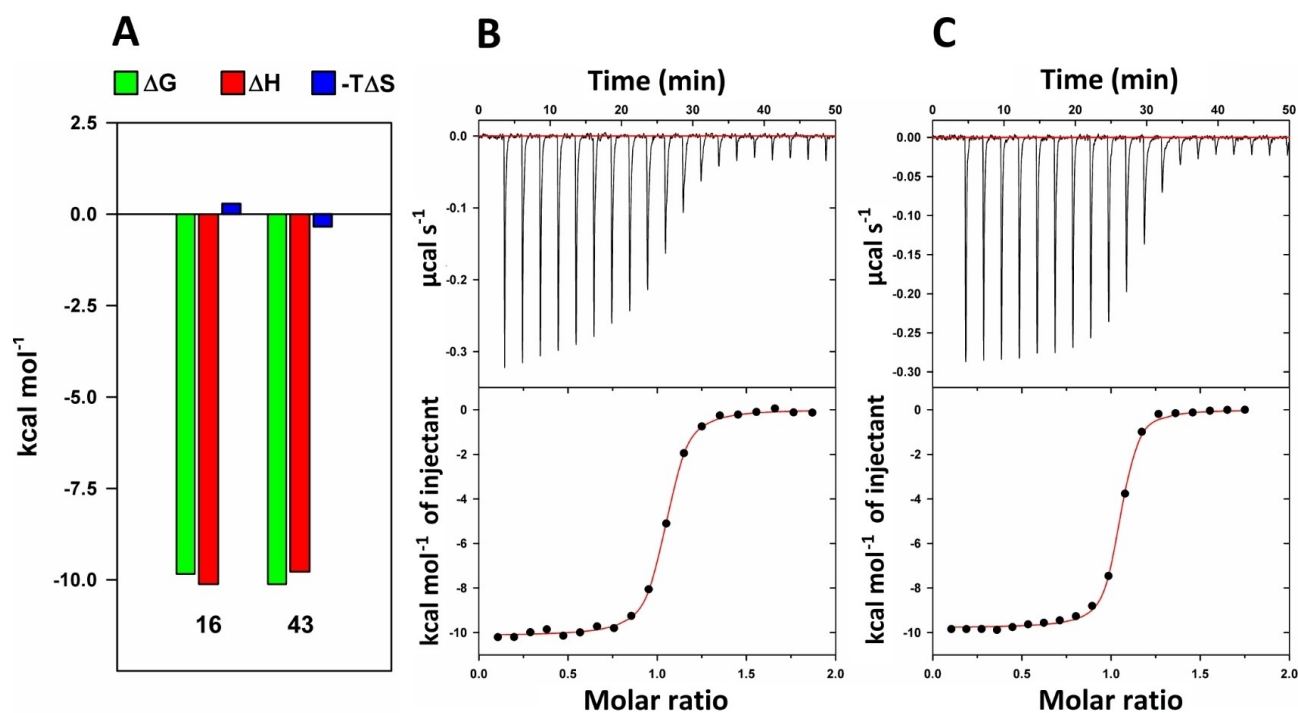
Table 2. Thermodynamic parameters of binding of compounds <b>16</b> and <b>43</b> to VIM-2 at 25 °C.						
Cpd	N <sup>[a]</sup>	K <sub>a</sub> (M <sup>-1</sup> ) <sup>[a]</sup>	K <sub>d</sub> [nM]	ΔG <sup>o</sup> <sub>b</sub> [kcal/mol]	ΔH <sup>o</sup> <sub>b</sub> <sup>[a]</sup> [kcal/mol]	TΔS <sup>o</sup> <sub>b</sub> [kcal/mol]
<b>16</b>	1.01 ± 0.01	1.6 ± 0.1 10 <sup>7</sup>	61	−9.8	−10.1 ± 0.1	−0.3
<b>43</b>	1.01 ± 0.01	2.6 ± 0.2 10 <sup>7</sup>	38	−10.1	−9.8 ± 0.1	0.3

[a] Values are mean ± SD.

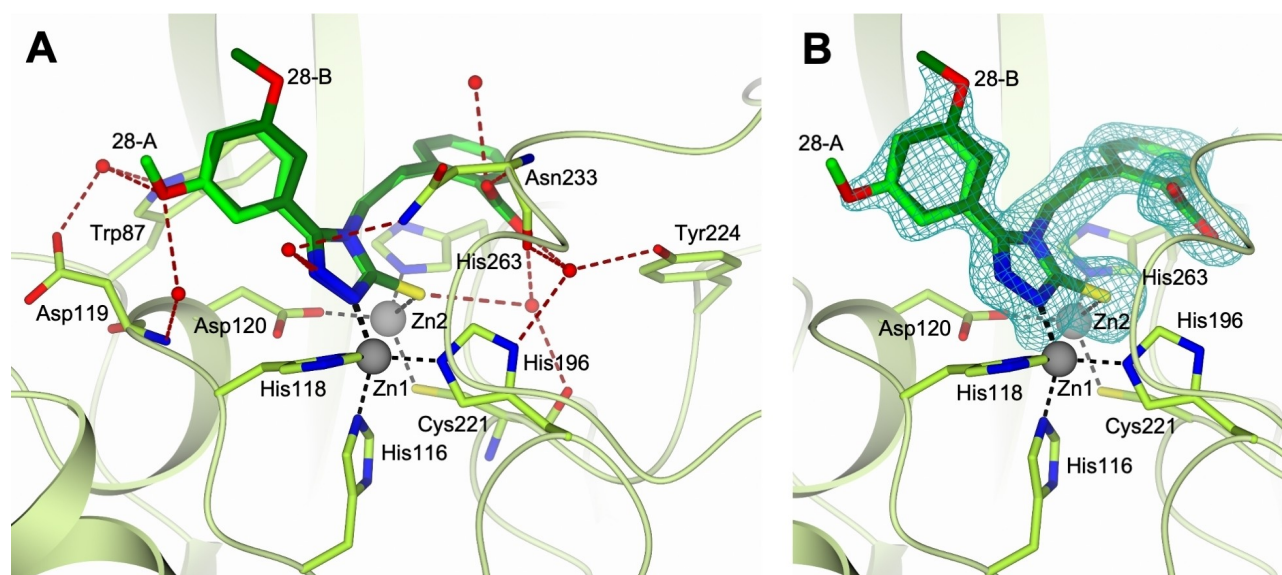
The experiment showed a stoichiometric relationship between VIM-2 and the inhibitors, which clearly indicated a 1:1 association. The two compounds behaved similarly with high enthalpy values, while the entropy value of compound **16** was slightly negative, in contrast to that of compound **43**. Compound binding was therefore enthalpy-driven (the enthalpy term is the major contributor to affinity). The favourable enthalpy contribution is an indication of specific interactions between binding partners and reflects ligand specificity and selectivity. The negative entropic term of compound **16** (unfavourable to ΔG<sup>o</sup><sub>b</sub>) is interpreted as a loss of degree of freedom due to reduction of accessible conformations of both molecules. By contrast, the positive entropic term of compound **43** (favourable to ΔG<sup>o</sup><sub>b</sub>) is regarded as resulting from the release of organized water molecules at the surfaces of individual partners to the bulk solvent.<sup>[50,51]</sup> Finally, in accordance with K<sub>i</sub> data, the study confirmed the higher VIM-2 inhibition potency of **16** and **43** compared to their hydrazone analogues (K<sub>d</sub> values of 61 and 38 nM, respectively, vs 519 and 68 nM<sup>[38]</sup>).

### Structural analysis of the VIM-2/28 complex

The crystal structure of VIM-2 in complex with compound **28**, one of the most potent VIM-2 inhibitors described herein, was obtained at 1.73 Å resolution (Figure 3, PDB code 7PP0). The structure showed that the triazole-thione core of the compound simultaneously coordinated both active site zinc ions, displacing the catalytic hydroxide anion (Figure 3A). The first zinc(II) ion, Zn1, is coordinated by the **28** nitrogen 2 and the three histidine residues of the 3H-site, His116, His118, and His196. The second zinc(II) ion, Zn2, is coordinated by the **28** thione and the three residues composing the DCH-site, Asp120, Cys221, and His263. The zinc-coordination bonds established by the inhibitor core are the same previously reported for other triazole-thione compounds in complex with L1,<sup>[36]</sup> VIM-2<sup>[37,38]</sup> or NDM-1.<sup>[39]</sup> The nitrogen in position 1 on the core forms water mediated H-bonds with the amide of Asn233. The thione group also entails water mediated interactions with the inhibitor carboxylate moiety (intramolecular interaction) and the backbone carbonyls



**Figure 2.** (A) VIM-2 binding energetics of compound 16 and 43. Data are from Table 2. (B) and (C) Isothermal titration calorimetry of VIM-2 by compounds 16 and 43 at 25 °C. Upper panel: exothermic microcalorimetric trace of compound injections into VIM-2 solution (18.7  $\mu$ M). Lower panel: Wiseman plot of heat releases versus molar ratio of injectant/protein in the cell and nonlinear fit of the binding isotherm for  $n$  equivalent binding sites. The binding enthalpy corresponds to the amplitude of the transition curve,  $K_d$  is derived from the slope of the transition and the stoichiometry  $n$  is determined at the transition midpoint.



**Figure 3.** Active site view of the structure of VIM-2 (light green cartoon and carbons, residues in sticks) in complex with 28 (in sticks, green and dark green carbons for the A and B-conformation, respectively). In the A panel, hydrogen and coordination bonds are represented as tan and black dashed lines, respectively, whereas in the B panel, the inhibitor is surrounded by the omit map (petrol mesh) contoured at the 3- $\sigma$  level. In all figures, Zn ions and water molecules are displayed as grey and red spheres (arbitrary radius), respectively. Oxygen atoms are coloured red, nitrogen blue, sulphur yellow (PDB code 7PP0).

of Cys221 and Asn233 (Figure 3A). The carboxylate of 28 is further stabilized through H-bond with the Asn233 backbone nitrogen and by additional water mediated interactions with

Tyr224 hydroxyl, His196 imidazole N $\delta$ 1, and Asn233 backbone carbonyl. The benzoic phenyl ring establishes a distorted  $\pi$ - $\pi$  interaction with the His263 imidazole. On the other side of the



catalytic cavity, the *m*-alkoxy phenyl substituent in position 5 adopts two alternate orientations inside the cavity (named as A and B in Figure 3A and B), mutually rotated by  $\sim 180^\circ$ . The phenyl moiety of both conformations is within van der Waals contact to the Trp87 indole. In the A-conformation, the oxygen of the *m*-alkoxy group forms water mediated H-bonds with the Trp87 indole nitrogen and with both the Asp119 carboxylate and backbone nitrogen (Figure 3A). Despite the interactions entailed by the *m*-alkoxy oxygen in the A conformation, they are probably not strong enough to stabilize the ring in a unique orientation, indeed it rotates by  $\sim 180^\circ$  in the B-conformation (Figure 3).

The terminal morpholine ring on the *m*-alkoxy group of **28** (both conformations) is located outside the catalytic cavity in the solvent exposed area, where it is characterized by positional disorder and thus excluded from our model (Figure 3). While the morpholinyl extension was added to establish additional interactions within the enzyme binding site, this result indicated that it was not the case and explained that compound **28** showed similar VIM-2 inhibitory potency as the corresponding methoxy-substituted compound **26**.

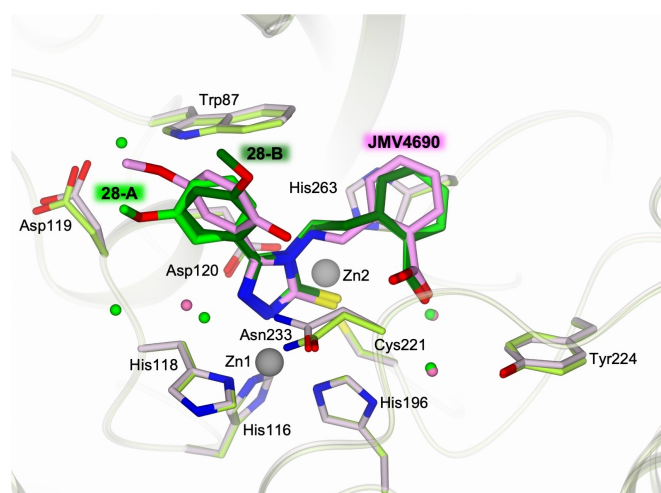
We formerly investigated other triazole-thione compounds, and reported the structural characterization of VIM-2 in complex with the Schiff base JMV4690 (PDB code 6YRP, compound **31** in reference [38]), which possesses a similar molecular structure to **28**. As expected, in addition to the conserved coordination bonds to the catalytic zinc ions, the comparison of the binding mode of JMV4690 with that of **28** highlights various common interactions within the VIM-2 active site (Figure 4). Both compounds have their benzoic moiety connected to the triazole-thione through a 2-atom linker. Despite the variable nature of this linker, their benzoic moiety shows the same orientation and interactions in the two complexes. On the other side of the cavity, a similar orientation is also observed for the phenyl of both compounds, that are mutually rotated by  $\sim 25^\circ$ . However, unlike compound

JMV4690 that forms a direct H-bond with the indole nitrogen of Trp87 through its *m*-methoxyl oxygen, the *m*-alkoxy oxygen of **28** (A-conformation) entails water mediated interactions with the same Trp87 and Asp119. Although flexible and therefore not defined in the modelled structure, the morpholinyl extension of **28** is a bulkier substituent that might prevent the same phenyl ring orientation as in JMV4690. In addition, the orientation of the phenyl in the complex with JMV4690 is further stabilized by the H-bond formed by its *o*-hydroxyl group with Asn233.

#### *In vitro* antibacterial synergistic activity.

Several compounds were selected to assess their ability to potentiate the activity of  $\beta$ -lactam antibiotics. First some were evaluated using a disk diffusion assay performed on two isogenic MBL-producing laboratory *Escherichia coli* strains (Table 3). AS19, a chemically mutagenized strain with enhanced permeability, or LZ2310, a triple knock-out mutant of K12 (in which genes encoding components of the major efflux pumps NorE, MdfA and AcrA were inactivated) were transformed with a derivative of the pLB-II plasmid in which the *bla*<sub>VIM-2</sub> gene was cloned.<sup>[52]</sup> The LZ2310 strain was used to limit the potential efflux of the compounds, which would prevent a sufficient inhibitor concentration to be established in the periplasm.

In this assay, the sub-micromolar or low micromolar VIM-2 inhibitors **16**, **21**, **27** and **34** were found to significantly potentiate the activity of cefoxitin against the VIM-2-producing LZ2310 strain (Table 3). Indeed, they restored susceptibility to the antibiotic, as a diameter of the growth inhibition zone of 20–24 mm (above the EUCAST resistance breakpoint, 18 mm) was measured. Compounds **31** and **38** were only moderately active although they were also sub-micromolar VIM-2 inhibitors, suggesting that they might be less able to efficiently cross the outer membrane and accumulate in the periplasm at biologically



**Figure 4.** Active site view of the superimposition between the structures of VIM-2 in complex with **28** (VIM-2 light green cartoon, carbons and waters; **28** in sticks, green and dark green carbons for the A and B-conformation, respectively, PDB code 7PP0) and compound JMV4690 (PDB code 6YRP;<sup>[38]</sup> VIM-2 light pink cartoon, carbons and waters; JMV4690 in sticks, pink carbons).

**Table 3.** *In vitro* synergistic activity of selected VIM-2 inhibitors measured by disk diffusion assay with hyperpermeable or efflux-deficient VIM-2-producing laboratory strains.<sup>[a]</sup>

Cpd <sup>[b]</sup>	$K_i$ [ $\mu$ M] on VIM-2 or (% inhibition at 100 $\mu$ M) <sup>[c]</sup>	Inhibition zone diameter [mm] <sup>[d]</sup>	
		AS19	LZ2310
None	–	16	11
EDTA	–	26	30
DMSO	–	17	10
<b>16</b>	0.25 $\pm$ 0.04	ND	21
<b>21</b>	0.58 $\pm$ 0.19	19	20
<b>24</b>	(40%)	17	9
<b>27</b>	0.15 $\pm$ 0.07	20	24
<b>31</b>	0.58 $\pm$ 0.19	19	18
<b>34</b>	1.07 $\pm$ 0.11	20	22
<b>38</b>	0.88 $\pm$ 0.06	17	15

[a] VIM-2-producing *E. coli* strains were obtained by transforming the pLBII-VIM-2 plasmid in strains AS19 (hyperpermeable strain) and LZ2310 (triple knock-out mutant of efflux pumps). [b] A variable volume of the compound dissolved in DMSO was added to a cefoxitin disk (30  $\mu$ g) to obtain a final inhibitor quantity of 40  $\mu$ g. DMSO was used as a control and did not affect the diameter of the growth inhibition zone. 220  $\mu$ g EDTA restored full susceptibility to the antibiotic. [c] From Table 1. [d] EUCAST resistance breakpoint = 18 mm. ND, not determined.

relevant concentrations. Finally, the moderate VIM-2 inhibitor **24** was completely inactive in these assays.

Compared to those obtained within the Schiff base series,<sup>[38]</sup> the present results were quite encouraging. Indeed, among the Schiff base analogues of **16**, **21** and **27**, only **16** was found active with a diameter of the growth inhibition zone equal to 20 mm.

In addition, although a more limited effect was observed on the VIM-2-producing AS19 strain, compounds **27** and **34** showed some detectable potentiation of cefoxitin.

Based on these results, the potential synergistic activity of a larger set of compounds (showing a  $K_i$  value for VIM-type enzymes  $\approx 10 \mu\text{M}$  or below) with meropenem was evaluated using a broth microdilution method on two multidrug-resistant clinical *K. pneumoniae* isolates producing either VIM-1 or VIM-4. Tested at a concentration of 32  $\mu\text{g}/\text{mL}$ , compounds were able to reduce the MIC of meropenem by 4 to 16-fold (Table 4). In particular, compound **43** displayed the highest activity against both isolates. Overall, a better synergistic activity was observed toward the VIM-4-producing clinical isolate, in agreement with the better inhibitory potencies of most tested inhibitors on VIM-4 rather than on VIM-1.

Compared to the Schiff base analogues,<sup>[38]</sup> which were devoid of activity in similar assays, and to the 4-alkanoic analogues,<sup>[45]</sup> which showed close activity in the same assays, these encouraging results confirmed that replacing the hydrazone-like bond by a non-hydrolysable one allowed to restore the susceptibility of MBL-producing clinical isolates to a carbapenem.

**Table 4.** Antibacterial synergistic activity of compounds on VIM-1 and VIM-4-producing *K. pneumoniae* clinical isolate with meropenem determined by the broth microdilution method.

Cpd (32 $\mu\text{g}/\text{mL}$ )	Meropenem MIC [ $\mu\text{g}/\text{mL}$ ]/ $K_i$ [ $\mu\text{M}$ ]			
	<i>K. pneumoniae</i> 7023 ( $bla_{\text{VIM-1}}$ )		<i>K. pneumoniae</i> VA-416/02 ( $bla_{\text{VIM-4}}$ )	
	MEM <sup>[a]</sup> MIC	$K_i$ (VIM-1) <sup>[b]</sup>	MEM <sup>[a]</sup> MIC	$K_i$ (VIM-4) <sup>[b]</sup>
None	16	–	16	–
<b>16</b>	8	NI	4	1.50 $\pm$ 0.15
<b>21</b>	8	6.41 $\pm$ 0.89	2	5.16 $\pm$ 0.44
<b>22</b>	4	12.4 $\pm$ 1.2	4	2.48 $\pm$ 0.24
<b>26</b>	8	7.65 $\pm$ 0.67	2	2.33 $\pm$ 0.10
<b>27</b>	16	7.55 $\pm$ 0.21	2	2.01 $\pm$ 0.13
<b>28</b>	4	4.69 $\pm$ 0.24	4	1.27 $\pm$ 0.06
<b>29</b>	4	1.60 $\pm$ 0.06	2	0.47 $\pm$ 0.01
<b>30</b>	4	4.67 $\pm$ 0.25	4	NI
<b>31</b>	4	8.08 $\pm$ 0.61	4	3.07 $\pm$ 0.31
<b>32</b>	8	15.5 $\pm$ 0.86	4	3.55 $\pm$ 0.35
<b>33</b>	16	10.2 $\pm$ 0.77	2	2.86 $\pm$ 0.19
<b>34</b>	8	NI	2	1.02 $\pm$ 0.06
<b>35</b>	16	8.71 $\pm$ 0.44	4	1.80 $\pm$ 0.12
<b>36</b>	8	9.19 $\pm$ 0.80	2	2.39 $\pm$ 0.14
<b>38</b>	16	NI	2	3.30 $\pm$ 0.28
<b>39</b>	8	6.07 $\pm$ 0.24	2	1.65 $\pm$ 0.13
<b>40</b>	8	11.5 $\pm$ 0.3	4	3.15 $\pm$ 0.17
<b>43</b>	2	1.61 $\pm$ 0.30	1	2.10 $\pm$ 0.54
<b>44</b>	4	(32%)	4	1.40 $\pm$ 0.27

[a] MEM, meropenem. [b] From Table 1. NI, no inhibition.

## Cytotoxicity assays on human cancer cells.

The potential cytotoxicity of compounds **21**, **31**, **34** and **43** was assessed using a membrane integrity assay (HeLa cells). They were found to not induce cell lysis at concentrations up to 250  $\mu\text{M}$ . This result was confirmed using a cell viability assay (HeLa cells, 1,500 cells/well), in which no cytotoxic effects could be observed after up to 72 h of incubation in the presence of 250  $\mu\text{M}$  of this compound.

## Conclusion

Schiff base analogues derived from 5-substituted-4-amino-1,2,4-triazole-3-thione derivatives were previously reported as broad-spectrum inhibitors of MBLs, including VIM-type enzymes, NDM-1, and, to a lesser extent, IMP-1.<sup>[38]</sup> However, they were devoid of synergistic activity when tested in clinical isolates in combination with a  $\beta$ -lactam antibiotic. The main reason was probably their poor penetration through the bacterial outer membrane and therefore their inability to accumulate at sufficient concentrations in the periplasm. Another reason could be the susceptibility of the hydrazone-like bond to hydrolysis. Based on the most potent Schiff base analogues, which possessed an *o*-benzoic acid at position 4, we decided to replace the hydrazone-like bond by a stable ethyl link. This change led to a narrower spectrum of inhibition. Indeed, although sub-micromolar to micromolar inhibitory potencies were maintained against VIM-type enzymes for many analogues, NDM-1 and IMP-1 were not or only poorly inhibited. The resulting change in geometry and flexibility was probably the main reason of this result, and these enzymes, in particular NDM-1, were not able to efficiently accommodate the different orientation of the 4-substituent with respect to the triazole ring. Concerning VIM-2 and VIM-4 inhibition, the study of substitution at position 5 confirmed the interest of several aryl moieties,<sup>[38,44,45]</sup> i.e. 2-hydroxy-4-methoxy-phenyl (**27**), some 5-membered heterocycles (**31**, **35**), naphthyl (**38**), *m*-biphenyl (**43**) and *p*-benzyloxyphenyl (**44**). In addition, two new  $R^1$  substituents possessing a cyclic amine-loaded ethoxy group at position 3 of the phenyl ring were also found favourable to VIM-type MBL inhibition (**28** and **29**). Compounds **28** and **29** are analogues of **26** (methoxy group at the same position as the ethoxy extension) and it is interesting to note that, while **28** similarly inhibited both VIM-type enzymes as **26**, **29** was a slightly better VIM-type MBL inhibitor. The 3D structure of **28** in the binding site of VIM-2 showed that only the methoxy portion of the flexible *N*-ethoxymorpholinyl extension was visible, possibly explaining why **28** was as potent as **26** against VIM-2. A structure of VIM-2 with **29** is not available, but it might be hypothesized that the *N*-methylpiperazine group is flexible and probably directed in the solvent exposed area, as the morpholine of **28**.

In contrast to the results obtained in the Schiff base series,<sup>[37]</sup> microbiological assays here identified several compounds able to potentiate the activity of a  $\beta$ -lactam antibiotic, not only when tested on two VIM-2-producing laboratory strains but also on two VIM-type MBL-producing clinical isolates of *K. pneumoniae*. Similar results were previously obtained for the 4-alkanoic series

(Figure 1C<sup>[44]</sup>), confirming the interest of replacing the hydrazone-like bond by a stable link. Finally, selected compounds did not show any cytotoxicity toward human cancer cells at high concentrations (i.e. 250  $\mu$ M).

Overall, although the best compounds displayed a spectrum of inhibition limited to VIM-type MBLs, the replacement of the potentially hydrolysable hydrazone-like bond of Schiff base analogues by a stable link was again found favourable to significantly improve the synergistic antibacterial activity in microbiological assays. Therefore, there is interest in pursuing the optimization of these MBL inhibitors, hopefully to obtain both broad-spectrum inhibitors and high antibiotic potentiation activity.

## Experimental Section

### Chemistry

#### General procedure for the preparation of 4-alkyl-1,2,4-triazole-3-thiones diversely substituted at position 5

The procedure followed the synthetic pathway reported by Deprez-Poulain *et al.*<sup>[47]</sup>

The hydrazone ( $R^1$ -CO-NHNH<sub>2</sub>) and amine ( $R^2$ -NH<sub>2</sub>) precursors were prepared as described in Supporting Information.

**Thiosemicarbazide intermediates.** To a solution of the amine  $R^2$ -NH<sub>2</sub> (1 mmol, 1 equiv.) in anhydrous DMF (4 mL) (in the case of hydrochloride salt, 1.5 equiv. of Na<sub>2</sub>CO<sub>3</sub> (159 mg) was added) was added DPT (244 mg, 1.05 mmol, 1.05 equiv.). The reaction mixture was stirred at 55 °C in a sealed tube for 1 h30. The hydrazone  $R^1$ -CONHNH<sub>2</sub> (1.1 mmol, 1.1 equiv.) was then added, and the mixture was again heated at 55 °C for 1 h30, and allowed to cool to room temperature. The solution was diluted in EtOAc and the organic phase was extracted five times with water, dried over MgSO<sub>4</sub> and concentrated in vacuum. If necessary, the product was purified by gel column chromatography (EtOAc/Hexane).

**Cyclization.** The thiosemicarbazide intermediates were solubilized in a mixture of water and ethanol (2:3, 2 mL/g) and KOH (3 equiv., 3 mmol) was added. The reaction mixture was refluxed for 2 h. The mixture was then neutralized with saturated aqueous KHSO<sub>4</sub> and extracted twice with DCM. The organic phases were mixed, dried over MgSO<sub>4</sub>, filtered and evaporated under vacuum. The residues were purified by gel column chromatography, recrystallization or RP HPLC (conditions indicated for each final compound in the Supporting Information). The purity of all compounds (excepted compounds **24** and **35**, which purity was about 91%) was determined to be  $\geq$  95%.

#### Isothermal titration calorimetry (ITC) analysis of compound binding to VIM-2

ITC titrations were performed on a MicroCal ITC200 (GE-Malvern) as previously described.<sup>[45]</sup>

#### X-ray crystallography

The VIM-2  $\beta$ -lactamase was purified and crystallized using the sitting drop method<sup>[53]</sup> at room temperature as previously described.<sup>[54–56]</sup>

The enzyme-inhibitor complex with compound **28** was obtained by the soaking method.<sup>[53]</sup> To perform this experiment, a 50 mM DMSO solution of **28** was formerly prepared and then diluted in PEG400 using a 1:9 molar ratio, right before compound addition to the crystallization drop. Crystals of the native enzyme were soaked with 1  $\mu$ L of this diluted solution, to reach a final inhibitor concentration of 5 mM in the crystallization drop. After 15 min, crystals were flash-frozen in liquid nitrogen. X-ray diffraction data were collected at 100 K using synchrotron radiation at the Diamond Light Source (DLS, Oxfordshire, UK) beamline I04, equipped with a Eiger2 XE 16 M detector. Reflections were integrated using XDS<sup>[57]</sup> and scaled with Scala<sup>[58]</sup> from the CCP4 suite.<sup>[59]</sup> The structure was solved by molecular replacement using the software Molrep<sup>[60]</sup> and the structure of VIM-2 (PDB code 6SP7<sup>[32]</sup>), as search model (excluding non-protein atoms and solvent molecules). Refinement was performed with REFMAC5<sup>[61]</sup> from the CCP4 suite, through an iterative manual rebuilding and modelling of missing atoms and solvent molecules in the electron density using Coot.<sup>[62]</sup> The inspection of the Fourier difference map clearly evidenced the presence of **28** inside the catalytic cavity of the enzyme that was modelled accordingly. The occupancy of the exogenous ligands (inhibitor and acetate anions) was adjusted and refined to values resulting in atomic displacement parameters in agreement with those of neighbouring protein atoms in fully occupied sites. The final model was manually inspected and validated with Coot and Procheck.<sup>[63]</sup> Structural figures were generated using the molecular graphic software CCP4 mg.<sup>[64]</sup> Data collection, processing and model refinement statistics are summarized in Table S1. Coordinates and structure factors for the VIM-2/**28** complex were deposited in the Protein Data Bank (<https://www.rcsb.org/>) under the code 7PP0.

### Biology

#### Metallo- $\beta$ -Lactamase inhibition assays

VIM-type enzymes, NDM-1 and IMP-1 were produced as previously described.<sup>[38]</sup>

The inhibition potency of the compounds has been assessed as previously reported.<sup>[38,44]</sup> Briefly, we measured the rate of hydrolysis of a reporter substrate (150  $\mu$ M imipenem or 150  $\mu$ M meropenem, absorbance variation followed at  $\lambda = 300$  nm) by a purified MBL enzyme (final concentration ranging from 1–70 nM) at 30 °C in 50 mM HEPES buffer (pH 7.5) in the absence and presence of several concentrations of the inhibitor (final concentration, 0.5–1,000  $\mu$ M).

The inhibition constants ( $K_i$ ) were determined on the basis of a model of competitive inhibition by analyzing the dependence of the ratio  $v_0/v_i$  ( $v_0$ , hydrolysis velocity in the absence of inhibitor;  $v_i$ , hydrolysis velocity in the presence of inhibitor) as a function of [I] as already described.<sup>[38,44,54]</sup> The assays were performed in triplicate.

#### Microbiological assays

The potential synergistic activity of selected compounds was first assessed by agar disk-diffusion method, according to the CLSI (Clinical Laboratory Standard Institute) recommendations, using Mueller-Hinton medium.<sup>[65]</sup> These tests were performed on MBL-producing isogenic laboratory strains obtained after transforming *Escherichia coli* LZ2310 (genotype,  $\Delta$ norE  $\Delta$ mdfA N43 acrA1)<sup>[66]</sup> and AS19<sup>[67]</sup> strains with a derivative of the high copy number plasmid pLB-II carrying the cloned *bla*<sub>VIM-2</sub> gene.

To ceftioxin (30  $\mu$ g)-containing disks (Oxoid, Milan, Italy) was added a solution of the inhibitor in DMSO (a maximum volume of 15  $\mu$ L was deposited on a disk to afford 40  $\mu$ g of compound). After incubation

at  $35 \pm 2^\circ\text{C}$  for 18 hours, the diameter of the growth inhibition zone was measured and compared to that obtained in the absence of inhibitor. DMSO and EDTA (220  $\mu\text{g}$ ) were used as negative and positive controls, respectively. Experiments were performed in triplicate.

Then, the minimum inhibitory concentrations (MICs) of meropenem were determined in triplicate using Mueller-Hinton broth and a bacterial inoculum of  $5 \times 10^4$  CFU/well, as recommended by the CLSI,<sup>[68]</sup> in both the absence and presence of a fixed concentration (32  $\mu\text{g}/\text{mL}$ ) of an inhibitor. The stock solutions of the antibiotic (1.2 mg/mL in sterile milliQ water) and compounds (3.2 mg/mL in DMSO) were diluted in the growth medium. For assessing the activity of the combination, the inhibitor was added at 32  $\mu\text{g}/\text{mL}$  to the wells immediately prior to the addition of the antibiotic diluted in growth medium containing 32  $\mu\text{g}/\text{mL}$  inhibitor and the two-fold serial dilutions. Multidrug resistant VIM-1- or VIM-4-producing *K. pneumoniae* clinical isolates present in our collection (7023 and VA-416/02, respectively<sup>[69,70]</sup>) were used and added extemporaneously to each well, prior to incubation of the plates at  $35^\circ\text{C}$  for 24 h. Results were read following visual inspection of the plates.

### Cell toxicity assay

The potential cytotoxic activity of selected compounds (21, 31, 34 and 43) was evaluated on HeLa cell cultures using the commercially available membrane integrity assay (CytoTox 96<sup>®</sup> non-radioactive cytotoxicity assay, Promega, Madison, WI, U.S.A.) as previously described.<sup>[38]</sup> The cytotoxicity of compounds was also assessed using the RealTime-Glo<sup>™</sup> MT Cell Viability Assay (Promega).<sup>[38]</sup> The assays were performed in triplicate.

### Abbreviations

CFU, colony-forming unit; CLSI, Clinical and Laboratory Standards Institute; DCM, dichloromethane; DMF, *N,N*-dimethylformamide; DMSO, dimethyl sulfoxide; DPT, di(2-pyridyl)thionocarbamate; EDTA, ethylenediaminetetraacetic acid; EtOAc, ethyl acetate; EUCAST, European Committee on Antimicrobial Susceptibility Testing; HeLa, tumoral cells from Henrietta Lacks; HEPES, 4-(2-hydroxyethyl)-1-piperazine-ethanesulfonic acid; IMP, imipenemase; ITC, isothermal calorimetry; KPC, *Klebsiella pneumoniae* carbapenemase; LC-MS, liquid chromatography coupled to mass spectrometry; MBL, metallo- $\beta$ -lactamase; MEM, meropenem; MIC, minimum inhibitory concentration; NDM, New Delhi metallo- $\beta$ -lactamase; OXA, oxacillinase; PDB, RCSB Protein Data Bank; SBL, serine- $\beta$ -lactamase; VIM, Verona integron-borne metallo- $\beta$ -lactamase.

### Acknowledgements

Part of this work was supported by Agence Nationale de la Recherche (ANR-14-CE16-0028-01, including fellowship to L.S.). We thank Mr. Pierre Sanchez for mass spectrometry analyses and Jean-Baptiste Masclef for technical assistance. Thanks are also due to Prof. Liam Good (Royal Veterinary College, London, U.K.) and Prof. Lynn Zechiedrich (Baylor College of Medicine, Houston, TX, USA) for providing the *E. coli* strains AS19 and LZ2310, respectively. We also thank the Diamond Light Source for providing us beamtime (BAG

proposal MX21741) and the staff of beamline I04 for their assistance with crystal testing and data collection. The Department of Medical Biotechnologies and the Department of Biotechnology, Chemistry and Pharmacy, University of Siena, were both awarded "Department of Excellence 2018–2022" by the Italian Ministry of Education, University and Research (MIUR, L. 232/2016).

### Conflict of Interest

The authors declare no conflict of interest.

### Data Availability Statement

The data that support the findings of this study are available from the corresponding author upon reasonable request.

**Keywords:** metallo- $\beta$ -lactamase inhibitors · 1,2,4-triazole-3-thiones · bacterial resistance ·  $\beta$ -lactam antibiotics

- [1] C. Lee Ventola, *Pharmacol. Ther.* **2015**, *40*, 277–283.
- [2] A. Cassini, L. D. Högberg, D. Plachouras, A. Quattrocchi, A. Hoxha, G. S. Simonsen, M. Colomb-Cotinac, M. E. Kretzschmar, B. Devleeschauwer, M. Cecchini, D. A. Ouakrim, T. C. Oliveira, M. J. Struelens, C. Suetens, D. L. Monnet, *Lancet Infect. Dis.* **2019**, *19*, 56–66.
- [3] World Health Organization, Global priority list of antibiotic-resistant bacteria to guide research, discovery and development of new antibiotics, 27 February 2017.
- [4] U. Theuretzbacher, K. Outtersson, A. Engel, A. Karlén, *Nat. Rev. Microbiol.* **2020**, *18*, 275–285.
- [5] P. Nordmann, T. Naas, L. Poirel, *Emerging Infect. Dis.* **2011**, *17*, 1791–1798.
- [6] T. R. Walsh, M. A. Toleman, *J. Antimicrob. Chemother.* **2012**, *67*, 1–3.
- [7] W. C. Reygaert, *AIMS Microbiol.* **2018**, *4*, 482–501.
- [8] K. Bush, *Antimicrob. Agents Chemother.* **2018**, *62*, e01076–18.
- [9] J.-D. Docquier, S. Mangani, *Drug Resist. Updates* **2018**, *36*, 13–29.
- [10] C. Gonzalez-Bello, D. Rodriguez, M. Pernas, A. Rodriguez, E. Colchon, *J. Med. Chem.* **2020**, *63*, 1859–1881.
- [11] T. Palzkill, *Ann. N. Y. Acad. Sci.* **2013**, *1277*, 91–104.
- [12] V. R. Gajamer, A. Bhattacharjee, D. Paul, C. Deshamukhya, A. K. Singh, N. Pradhan, H. K. Tiwari, *J. Glob. Antimicrob. Resist.* **2018**, *14*, 228–232.
- [13] M. J. Martin, B. W. Corey, F. Sannio, L. R. Hall, U. MacDonald, B. T. Jones, E. G. Mills, C. Harless, J. Stam, R. Maybank, Y. Kwak, K. Schaufler, K. Becker, N. O. Hübner, S. Cresti, G. Tordini, M. Valassina, M. G. Cusi, J. W. Bennett, T. A. Russo, P. T. McGann, F. Lebreton, J. D. Docquier, *Proc. Natl. Acad. Sci. USA* **2021**, *118*, e2110227118.
- [14] R. P. McGeary, D. T. Tan, G. Schenk, *Future Med. Chem.* **2017**, *9*, 673–691.
- [15] A. R. Palacios, M.-A. Rossi, G. S. Mahler, A. J. Vila, *Biomolecules* **2020**, *10*, 854.
- [16] A. Y. Chen, R. N. Adamek, B. L. Dick, C. V. Credille, C. N. Morrison, S. M. Cohen, *Chem. Rev.* **2019**, *119*, 1323–1455.
- [17] B. M. Liénard, G. Garau, L. Horsfall, A. I. Karsiotis, C. Damblon, P. Lassaux, C. Papamichael, G. C. Roberts, M. Galleni, O. Dideberg, J.-M. Frère, C. J. Schofield, *Org. Biomol. Chem.* **2008**, *6*, 2282–2294.
- [18] P. Lassaux, M. Hamel, M. Gulea, H. Delbrück, P. S. Mercuri, L. Horsfall, D. Dehareng, M. Kupper, J.-M. Frère, K. Hoffmann, M. Galleni, C. Bebrone, *J. Med. Chem.* **2010**, *53*, 4862–4876.
- [19] M. M. Gonzalez, M. Kosmopoulou, M. F. Mojica, V. Castillo, P. Hinchliffe, I. Pettinati, J. Brem, C. J. Schofield, G. Mahler, R. A. Bonomo, L. I. Llarrull, J. Spencer, A. J. Vila, *ACS Infect. Dis.* **2015**, *1*, 544–554.
- [20] J. H. Toney, G. G. Hammond, P. M. Fitzgerald, N. Sharma, J. M. Balkovec, G. P. Rouen, S. H. Olson, M. L. Hammond, M. L. Greenlee, Y. D. Gao, *J. Biol. Chem.* **2001**, *276*, 31913–31918.
- [21] A. Y. Chen, P. W. Thomas, A. C. Stewart, A. Bergstrom, Z. Cheng, C. Miller, C. R. Bethel, S. H. Marshall, C. V. Credille, C. L. Riley, R. C. Page, R. A.

- Bonomo, M. W. Crowder, D. L. Tierney, W. Fast, S. M. Cohen, *J. Med. Chem.* **2017**, *60*, 7267–7283.
- [22] A. M. King, S. A. Reid-Yu, W. Wang, D. T. King, G. De Pascale, N. C. Strynadka, T. R. Walsh, B. K. Coombes, G. D. Wright, *Nature* **2014**, *510*, 503–506.
- [23] A. Bergstrom, A. Katko, Z. Adkins, J. Hill, Z. Cheng, M. Burnett, H. Yang, M. Aitha, M. R. Mehaffey, J. S. Brodbelt, K. H. Tehrani, N. I. Martin, R. A. Bonomo, R. C. Page, D. L. Tierney, W. Fast, G. D. Wright, M. W. Crowder, *ACS Infect. Dis.* **2018**, *4*, 135–145.
- [24] A. Matsuura, H. Okumura, R. Asakura, N. Ashizawa, M. Takahashi, F. Kobayashi, N. Ashikawa, K. Arai, *Jpn. J. Pharmacol.* **1993**, *63*, 187–193.
- [25] O. Samuelsen, O. A. H. Astrand, C. Fröhlich, A. Heikal, S. Skagseth, T. J. O. Carlsen, H. S. Leiros, A. Bayer, C. Schnaars, G. Kildahl-Andersen, S. Lauksund, S. Finke, S. Huber, T. Gjoen, A. M. S. Andresen, O. A. Okstad, P. Rongved, *Antimicrob. Agents Chemother.* **2020**, *64*:e02415–19.
- [26] N. Reddy, M. Shungube, P. I. Arvidsson, S. Bajinath, H. G. Kruger, T. Goverder, T. Naicker, *Expert Opin. Ther. Pat.* **2020**, *30*, 541–555.
- [27] D. T. Davies, S. Leiris, N. Sprynski, J. Castandet, C. Lozano, J. Bousquet, M. Zalacain, S. Vasa, P. K. Dasari, R. Pattipati, N. Vempala, S. Gujjewar, S. Godi, R. Jallala, R. S. Sathyap, N. A. Darshanoju, V. R. Ravu, R. R. Juvenhala, N. Pottabathini, S. Sharma, S. Pothukanuri, K. Holden, P. Warn, F. Marcocchia, M. Benvenuti, C. Pozzi, S. Mangani, J.-D. Docquier, M. Lemonnier, M. Everett, *ACS Infect. Dis.* **2020**, *6*, 2419–2430.
- [28] C. J. Burns, D. Daigle, B. Liu, D. McGarry, D. C. Pevear, R. E. Trout (Venatorx Pharmaceuticals), WO 2014/089365 A1, **2014**.
- [29] J. Brem, R. Cain, S. Cahill, M. A. McDonough, I. J. Clifton, J. C. Jiménez-Castellanos, M. B. Avison, J. Spencer, C. W. Fishwick, C. J. Schofield, *Nat. Commun.* **2016**, *7*, 12406.
- [30] A. Krajnc, J. Brem, P. Hinchliffe, K. Calvopiña, T. D. Panduwawala, P. A. Lang, J. J. A. G. Kamps, J. M. Tyrrell, E. Widlake, B. G. Seward, T. R. Walsh, J. Spencer, C. J. Schofield, *J. Med. Chem.* **2019**, *62*, 8544–8556.
- [31] J. C. Hamrick, J.-D. Docquier, T. Uehara, C. L. Myers, D. A. Six, C. L. Chatwin, K. J. John, S. F. Vernacchio, S. M. Cusick, R. E. L. Trout, C. Pozzi, F. De Luca, M. Benvenuti, S. Mangani, B. Liu, R. W. Jackson, G. Moeck, L. Xerri, C. J. Burns, D. C. Pevear, D. M. Daigle, *Antimicrob. Agents Chemother.* **2020**, *64*: e01963–19.
- [32] B. Liu, R. E. L. Trout, G. H. Chu, D. McGarry, R. W. Jackson, J. C. Hamrick, D. M. Daigle, S. M. Cusick, C. Pozzi, F. De Luca, M. Benvenuti, S. Mangani, J.-D. Docquier, W. J. Weis, D. C. Pevear, L. Xerri, C. J. Burns, *J. Med. Chem.* **2020**, *63*, 2789–2801.
- [33] S. J. Hecker, K. R. Reddy, O. Lomovskaya, D. C. Griffith, D. Rubio-Aparicio, K. Nelson, R. Tsvikovski, D. Sun, M. Sabet, Z. Tarazi, J. Parkinson, M. Totrov, S. H. Boyer, T. W. Glinka, O. A. Pemberton, Y. Chen, M. N. Dudley, *J. Med. Chem.* **2020**, *63*, 7491–7507.
- [34] K. Nelson, D. Rubio-Aparicio, R. Tsvikovski, D. Sun, M. Totrov, M. Dudley, O. Lomovskaya, *Antimicrob. Agents Chemother.* **2020**, *64*: e01406–20.
- [35] J. C. Vasquez-Ucha, J. Arca-Suarez, G. Bou, A. Beceiro, *Int. J. Mol. Sci.* **2020**, *21*, 9308.
- [36] L. Nauton, R. Kahn, G. Garau, J.-F. Hernandez, O. Dideberg, *J. Mol. Biol.* **2008**, *375*, 257–269.
- [37] T. Christopet, T. J. Carlsen, R. Helland, H. K. Leiros, *J. Med. Chem.* **2015**, *58*, 8671–8682.
- [38] L. Gavara, L. Seville, F. De Luca, P. Mercuri, C. Bebrone, G. Feller, A. Legru, G. Cerboni, S. Tanfoni, D. Baud, G. Cutolo, B. Bestgen, G. Chelini, F. Verdirosa, F. Sannio, C. Pozzi, M. Benvenuti, K. Kwapien, M. Fischer, K. Becker, J.-M. Frère, S. Mangani, N. Gresh, D. Berthomieu, M. Galleni, J.-D. Docquier, J.-F. Hernandez, *Eur. J. Med. Chem.* **2020**, *208*, 112720.
- [39] F. Spyrikis, M. Santucci, L. Maso, S. Cross, E. Gianquinto, F. Sannio, F. Verdirosa, F. De Luca, J.-D. Docquier, L. Cendron, D. Tondi, A. Venturini, G. Cruciani, M. P. Costi, *Sci. Rep.* **2020**, *10*, 12763.
- [40] L. Olsen, S. Jost, H. W. Adolph, I. Petterson, L. Hemmingsen, F. S. Jørgensen, *Bioorg. Med. Chem.* **2006**, *14*, 2627–2635.
- [41] P. Vella, W. M. Hussein, E. W. Leung, D. Clayton, D. L. Ollis, N. Mitic, G. Schenk, R. P. McGeary, *Bioorg. Med. Chem. Lett.* **2011**, *21*, 3282–3285.
- [42] F. Spyrikis, G. Celenza, F. Marcocchia, M. Santucci, S. Cross, P. Bellio, L. Cendron, M. Perilli, D. Tondi, *ACS Med. Chem. Lett.* **2018**, *9*, 45–50.
- [43] L. Seville, L. Gavara, C. Bebrone, F. De Luca, L. Nauton, M. Achard, P. Mercuri, S. Tanfoni, L. Borgianni, C. Guyon, P. Lonjon, G. Turan-Zitouni, J. Dzieciolowski, K. Becker, L. Bénard, C. Condon, L. Maillard, J. Martinez, J.-M. Frère, O. Dideberg, M. Galleni, J.-D. Docquier, J.-F. Hernandez, *ChemMedChem* **2017**, *12*, 972–985.
- [44] L. Gavara, F. Verdirosa, A. Legru, P. S. Mercuri, L. Nauton, L. Seville, G. Feller, D. Berthomieu, F. Sannio, F. Marcocchia, S. Tanfoni, F. De Luca, N. Gresh, M. Galleni, J.-D. Docquier, J.-F. Hernandez, *Biomolecules* **2020**, *10*, 1094.
- [45] L. Gavara, A. Legru, F. Verdirosa, L. Seville, L. Nauton, G. Corsica, P. S. Mercuri, F. Sannio, G. Feller, R. Coulon, F. De Luca, G. Cerboni, S. Tanfoni, G. Chelini, M. Galleni, J.-D. Docquier, J.-F. Hernandez, *Bioorg. Chem.* **2021**, *113*, 105024.
- [46] A. Legru, F. Verdirosa, J.-F. Hernandez, G. Tassone, F. Sannio, M. Benvenuti, P.-A. Conde, G. Bossis, C. A. Thomas, M. W. Crowder, M. Dillenberger, K. Becker, C. Pozzi, S. Mangani, J.-D. Docquier, L. Gavara, *Eur. J. Med. Chem.* **2021**, *226*, 113873.
- [47] R. F. Deprez-Poulain, J. Charton, V. Leroux, B. P. Deprez, *Tetrahedron Lett.* **2007**, *48*, 8157–8162.
- [48] U. R. Mach, A. E. Hackling, S. Perachon, S. Ferry, C. G. Wermuth, J.-C. Schwartz, P. Sokoloff, H. Stark, *ChemBioChem* **2004**, *5*, 508–518.
- [49] J. Stephen Clark, P. B. Hodgson, M. D. Goldsmith, L. J. Street, *J. Chem. Soc. Perkin Trans. 1* **2001**, 3312–3324.
- [50] E. Freire, *Drug Discovery Today* **2008**, *13*, 869–874.
- [51] J. E. Ladbury, *Biochem. Soc. Trans.* **2010**, *38*, 888–893.
- [52] L. Borgianni, J. Vandenamee, A. Matagne, L. Bini, R. Bonomo, J.-M. Frère, G. M. Rossolini, J.-D. Docquier, *Antimicrob. Agents Chemother.* **2010**, *54*, 3197–3204.
- [53] M. Benvenuti, S. Mangani, *Nat. Protoc.* **2007**, *2*, 1633–1651.
- [54] J.-D. Docquier, J. Lamotte-Brasseur, M. Galleni, G. Amicosante, J. M. Frère, G. M. Rossolini, *J. Antimicrob. Chemother.* **2003**, *51*, 257–266.
- [55] I. Garcia-Saez, J.-D. Docquier, G. M. Rossolini, O. Dideberg, *J. Mol. Biol.* **2008**, *375*, 604–611.
- [56] S. Leiris, A. Coelho, J. Castandet, M. Bayet, C. Lozano, J. Bougnon, J. Bousquet, M. Everett, M. Lemonnier, N. Sprynski, M. Zalacain, T. D. Pallin, M. C. Cramp, N. Jennings, G. Raphy, M. W. Jones, R. Pattipati, B. Shankar, R. Sivasubrahmanyam, A. K. Soodhagani, R. R. Juvenhala, N. Pottabathini, S. Pothukanuri, M. Benvenuti, C. Pozzi, S. Mangani, F. De Luca, G. Cerboni, J.-D. Docquier, D. T. Davies, *ACS Infect. Dis.* **2019**, *5*, 131–140.
- [57] W. Kabsch, *Acta Crystallogr. Sect. D* **2010**, *66*, 125–132.
- [58] P. R. Evans, *Acta Crystallogr. Sect. D* **2011**, *67*, 282–292.
- [59] M. D. Wynn, C. C. Ballard, K. D. Cowtan, E. J. Dodson, P. Emsley, P. R. Evans, R. M. Keegan, E. B. Krissinel, A. G. Leslie, A. McCoy, S. J. McNicholas, G. N. Murshudov, N. S. Pannu, E. A. Potterton, H. R. Powell, R. J. Read, A. Vagin, K. S. Wilson, *Acta Crystallogr. Sect. D* **2011**, *67*, 235–242.
- [60] A. Vagin, A. Teplyakov, *Acta Crystallogr. Sect. D* **2010**, *66*, 22–25.
- [61] G. N. Murshudov, P. Shubak, A. A. Lebedev, N. S. Pannu, R. A. Steiner, R. A. Nicholls, M. D. Winn, F. Long, A. A. Vagin, *Acta Crystallogr. Sect. D* **2011**, *67*, 355–367.
- [62] P. Emsley, B. Lohkamp, W. G. Scott, K. Cowtan, *Acta Crystallogr. Sect. D* **2010**, *66*, 486–501.
- [63] R. A. Laskowski, M. W. MacArthur, D. S. Moss, J. M. Thornton, *J. Appl. Crystallogr.* **1993**, *26*, 283–291.
- [64] S. McNicholas, E. Potterton, K. S. Wilson, M. E. M. Noble, *Acta Crystallogr. Sect. D* **2011**, *67*, 386–394.
- [65] Clinical Laboratory Standard Institute, Performance standards for antimicrobial disk susceptibility tests; approved standard, Document M02-A12, 2015, Twelfth Edition, Wayne, PA, USA.
- [66] S. Yang, S. R. Clayton, E. L. Zechiedrich, *J. Antimicrob. Chemother.* **2003**, *51*, 545–556.
- [67] M. Sekiguchi, S. Iida, *Proc. Natl. Acad. Sci. USA* **1967**, *58*, 2315–2320.
- [68] Clinical Laboratory Standard Institute, Methods for dilution antimicrobial susceptibility tests for bacteria that grow aerobically, Document M07-A10, 2015, Twelfth Edition, Wayne, PA, USA.
- [69] S. Cagnacci, L. Gualco, S. Roveta, S. Mannelli, L. Borgianni, J.-D. Docquier, F. Dodi, M. Centanaro, E. Debbia, A. Marchese, G. M. Rossolini, *J. Antimicrob. Chemother.* **2008**, *61*, 296–300.
- [70] F. Luzzaro, J.-D. Docquier, C. Colinon, A. Endimiani, G. Lombardi, G. Amicosante, G. M. Rossolini, A. Toniolo, *Antimicrob. Agents Chemother.* **2004**, *48*, 648–650.

Manuscript received: November 5, 2021

Revised manuscript received: December 27, 2021

Accepted manuscript online: January 20, 2022

Version of record online: February 4, 2022